3.2.4 Energy correction for Bremsstrahlung.

At $\sqrt{s} = 172$ GeV, the search for energy deposits from Bremsstrahlung photons uses a cone, with an opening angle of 2°, around the electron impact point on ECAL. No check is made on the isolation of the electron, with the result that a lot of energy is added to the electron candidate track in background events.

In order to investigate whether an opening angle of 2° is the optimal choice, the bias and resolution on the electron energy are studied for several opening angles. Figure 3.22 shows the bias and resolution, which are defined to be the mean and RMS of the distribution of the reconstructed electron energy minus the true electron energy, known from simulation. Only events in which the electron in $e\bar{\nu}q\bar{q}$ events is correctly identified by the missing momentum technique are studied here. The results are separated into four classes:

- $e\bar{\nu}q\bar{q}$ events with neither Bremsstrahlung nor Final State Radiation (FSR) from the electron.
- $e\bar{\nu}q\bar{q}$ events with Bremsstrahlung but without FSR from the electron.
- $e\bar{\nu}q\bar{q}$ events without Bremsstrahlung but with FSR from the electron.
- $e\bar{\nu}q\bar{q}$ events with Bremsstrahlung and with FSR from the electron (not shown).

With no correction at all, *ie* an opening angle of 0°, the electron energy is underestimated by over 5 GeV on average for events with Bremsstrahlung and the resolution on the electron energy is 9 GeV instead of 1.6 GeV. As the opening angle is increased, the average bias goes down to -0.7 GeV and the resolution improves to just under 3 GeV. The optimal choice for the opening angle is in the range 2°- 3°. In order to improve the resolution slightly for events with FSR, the opening angle is chosen to be 2.5°.

In order to reduce the amount of energy added to the electron candidate track in background events, the amount of charged energy within 6° of the electron track is required to be less than 5 GeV. This is designed to keep the Bremsstrahlung correction for 99% of the signal $W^+W^-\rightarrow e\bar{\nu}q\bar{q}$ events and to reduce the percentage of $Z/\gamma\rightarrow q\bar{q}(\gamma)$ events to which the correction is applied, in this case to 53%.

During the development of the $\sqrt{s} = 183$ GeV analysis, the simple weighting of the tracking and calorimeter estimates for the electron four-vector was found to bias the direction of the electron. The tracking actually gives the best estimate for the original

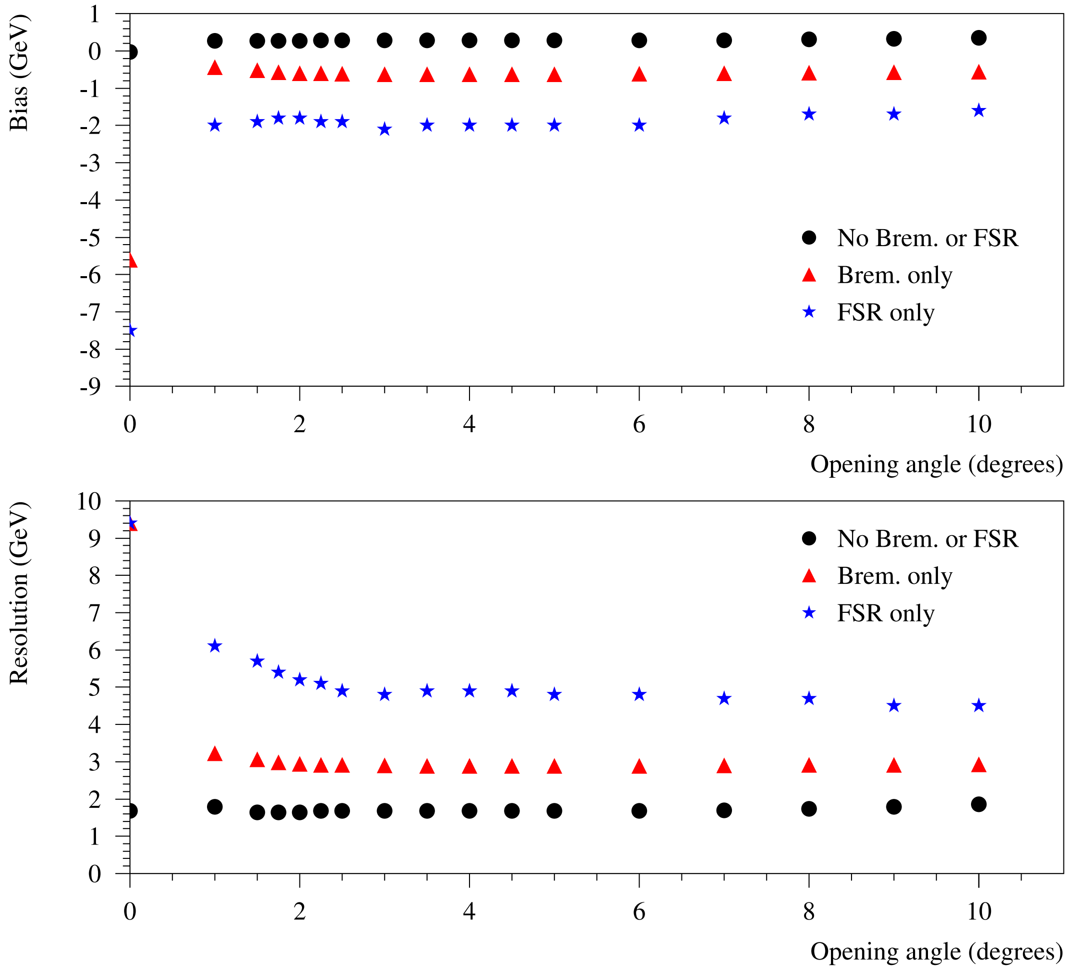

Figure 3.22: The variation of the bias (top) and resolution (bottom) on the electron energy for several values of the opening angle.

electron direction due to the importance of the high precision coordinates from the VDET in the track helix fit. As the majority of the Bremsstrahlung radiation occurs after the electron has passed through the VDET, the VDET coordinates are on the original trajectory of the electron. Therefore, the electron energy is corrected as before, but the tracking estimate for the direction is kept and the electron track momentum is simply scaled in order to set the electron mass:

$$\begin{aligned} E_{corr} &= w_{track} E_{track} + w_{cal} E_{cal} \\ \mathbf{p}_{corr} &= \frac{\sqrt{E_{corr}^2 - m_e^2}}{|\mathbf{p}_{track}|} \mathbf{p}_{track} \end{aligned} \tag{3.21}$$

3.2.5 Search for Final State Radiation.

Final State Radiation occurs as a result of the acceleration of a charge during the decay of the W boson. In the KORALW program, FSR is modelled by PHOTOS [58]. FSR, of up to two photons, happens in 18% of all simulated $W \rightarrow e\bar{\nu}$ decays and 10% of all simulated $W \rightarrow \mu\bar{\nu}$ decays, with a mean photon energy of 8 GeV. The photons may be radiated at large angles with respect to the lepton, though 90% are within 30° of the lepton. Some of the photons are recovered by the Bremsstrahlung correction, but the remainder are mistakenly included in the jet clustering. This can seriously bias the jet direction and energy and can give an equal mass constraint kinematic fit severe problems.

In order to improve the event reconstruction, a search is made for FSR [84]. Figure 3.23 shows a display of a simulated $\mu\bar{\nu}q\bar{q}$ event with FSR. The energy deposit in ECAL from the photon is clearly visible and is easily identified as a photon by the GAMPEX program [85]. Therefore, the closest GAMPEX photon to the lepton that meets the following criteria is considered as an FSR candidate:

- Energy greater than 0.5 GeV.
- Inconsistent with a $\pi^0 \rightarrow \gamma\gamma$ hypothesis from QPI0DO [86].
- Not associated to any object found by the Bremsstrahlung correction.

In order to avoid photons that are from the hadronic jets or from ISR, the following three requirements, illustrated in Figure 3.24, must be satisfied:

- The photon must be more than 40° away from the nearest good charged track that is not the lepton. In simulated events, 95% of the photons from the hadronic jets are within 40° of a good charged track that is not the lepton.
- The photon must be closer to the lepton than to the beam axis. In simulated events, 70% of all ISR photons are within 20° of the beam axis. Note also that photon identification extends down to 12° from the beam axis and that the lepton must be at least 18° away from the beam axis.
- The photon must be closer to the lepton than to any other charged track.

The four-vector of the FSR candidate is then added to the tracking estimate of the lepton four-vector. This is different to the Bremsstrahlung case as FSR occurs essentially at the

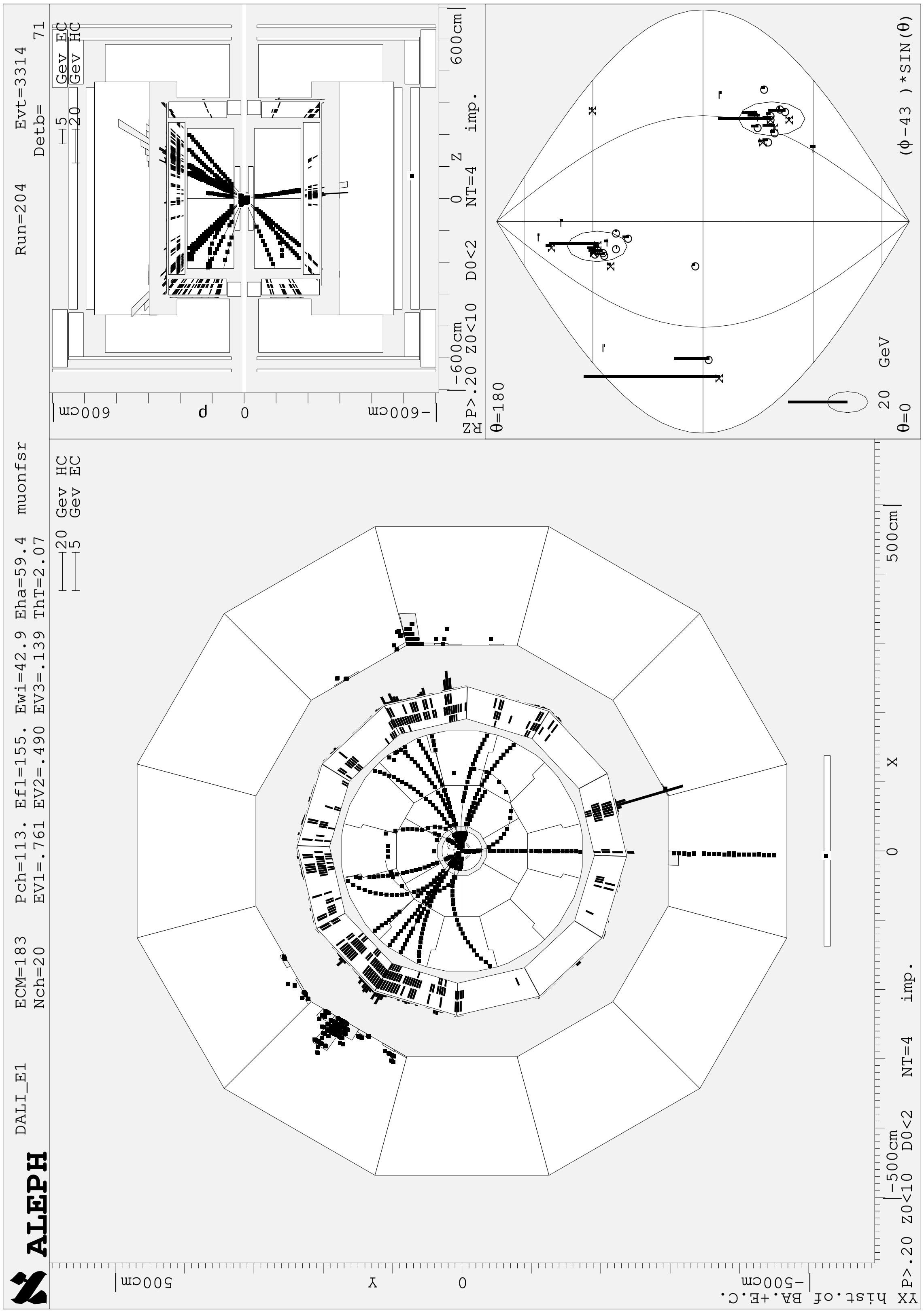

Figure 3.23: Event display for a simulated $e^+e^-\!\to\!W^+W^-\!\to\!\mu\bar{\nu}q\bar{q}$ decay with FSR from the muon

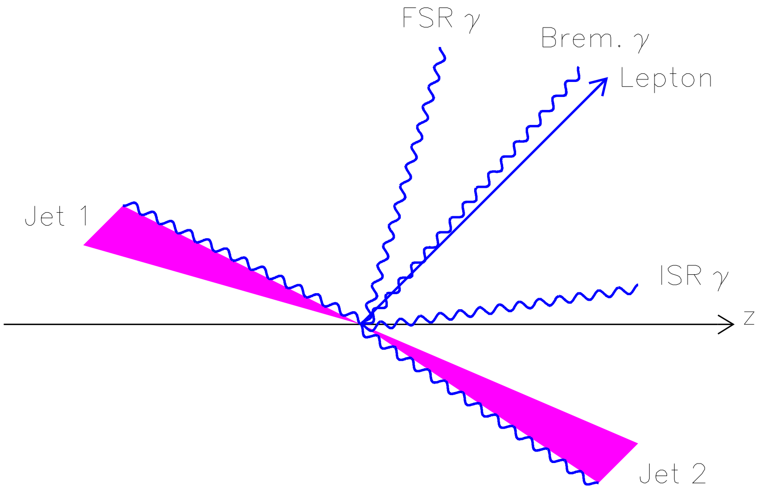

Figure 3.24: Schematic of photons in a $W^+W^- \rightarrow e\bar{\nu}q\bar{q}$ decay.

interaction point and may subtend a wide angle with respect to the lepton. Therefore, the tracking estimate of the lepton direction does not, in general, closely correspond to the original lepton direction.

As photons are not identified close to charged tracks with high efficiency, any energy deposit over 2 GeV that is found in the Bremsstrahlung region is added to the muon track energy in order to improve the reconstruction of the muon energy. The isolation check described in the previous section is also made for the muon.

The performance of the combined Bremsstrahlung correction and FSR search is shown in Table 3.11. The correction is applied to 39% and 9% of simulated $e\bar{\nu}q\bar{q}$ and $\mu\bar{\nu}q\bar{q}$ events, respectively. After subtracting the percentage of events without any photon radiation but to which the correction is mistakenly applied, about 45% of all FSR photons are recovered, increasing to 60% for FSR photon energies above 5 GeV. Around 32% of the Bremsstrahlung photons are found, which increases to 71% for Bremsstrahlung photon energies over 5 GeV. Energy is mistakenly added to the lepton in 18% and 4% of $e\bar{\nu}q\bar{q}$ and $\mu\bar{\nu}q\bar{q}$ events, respectively, but the average energy added is much less at 2 GeV. The correction is applied to 18% of the simulated $Z/\gamma \rightarrow q\bar{q}(\gamma)$ events selected in the $e\bar{\nu}q\bar{q}$ channel and only 9% of those selected in the $\mu\bar{\nu}q\bar{q}$ channel.

Figures 3.25 and 3.26 show the resolution on the lepton energy before and after the Bremsstrahlung correction and FSR search for leptons with and without energy lost to photon radiation. The resolution on the lepton energy, in those events that do not have any

Process	Composition	Percentage with energy added	Mean energy added (GeV)
$e^+e^-\to W^+W^-\to e\bar{\nu}q\bar{q}$	100	39	9.4
No Brem. or FSR	40	18	1.6
Brem. only	44	50	10.8
E_{Brem} >5 GeV	14	89	16.8
FSR only	9	59	10.8
E_{FSR} >5 GeV	4	78	17.1
$e^+e^-\to Z/\gamma\to q\bar{q}(\gamma)$	100	18	15.7
$e^+e^-\to W^+W^-\to \mu\bar{\nu}q\bar{q}$	100	8	5.1
No FSR	91	4	2.3
FSR	9	54	7.1
E_{FSR} >5 GeV	3	65	13.6
$e^+e^-\to Z/\gamma\to q\bar{q}(\gamma)$	100	9	10.6

Table 3.11: Mean energy added by the combined Bremsstrahlung correction and FSR search to fully simulated, selected $W^+W^-\to e\bar{\nu}q\bar{q}$ and $e^+e^-\to Z/\gamma\to q\bar{q}(\gamma)$ events. The second column breaks the sample down into various components and the third column gives the percentage of that component to which energy is added.

energy lost to photon radiation, is not significantly worsened by the corrections, although the energy is biased upwards by 0.2 GeV on average for electrons. The overall resolution on the electron energy improves to 4.2 GeV from 8.7 GeV and the bias decreases to -0.8 GeV from -4.3 GeV. The overall resolution on the muon energy also improves to 3.1 GeV from 3.8 GeV and the bias decreases to -0.2 GeV from -0.6 GeV. The energy added by the Bremsstrahlung correction and FSR search is shown in Figure 3.27 for data and simulation. The agreement between them is good.

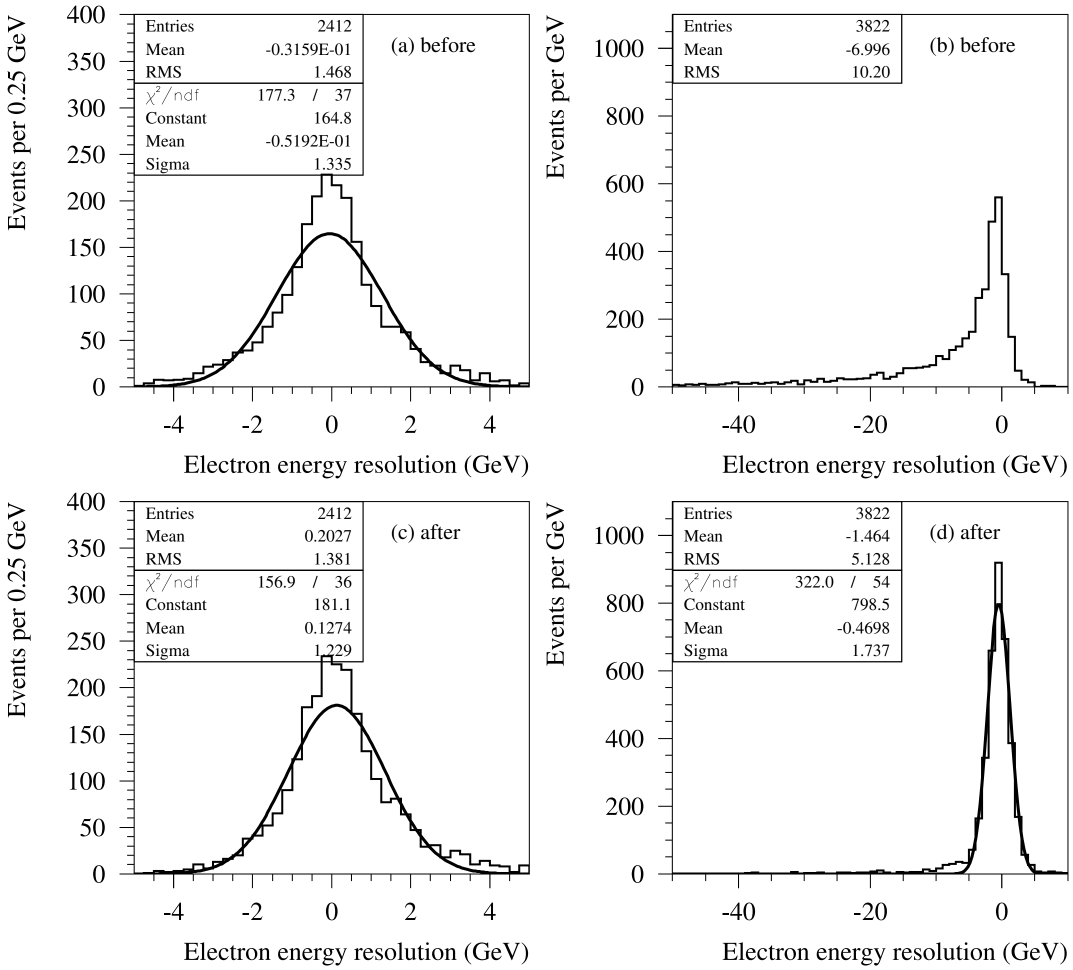

Figure 3.25: The resolution on the electron energy, in fully simulated and selected $e\bar{\nu}q\bar{q}$ events, before the Bremsstrahlung correction and FSR search for (a) events without any energy lost to photon radiation and (b) events with some energy lost to photon radiation. The corresponding resolutions after the Bremsstrahlung correction and FSR search are shown in (c) and (d).

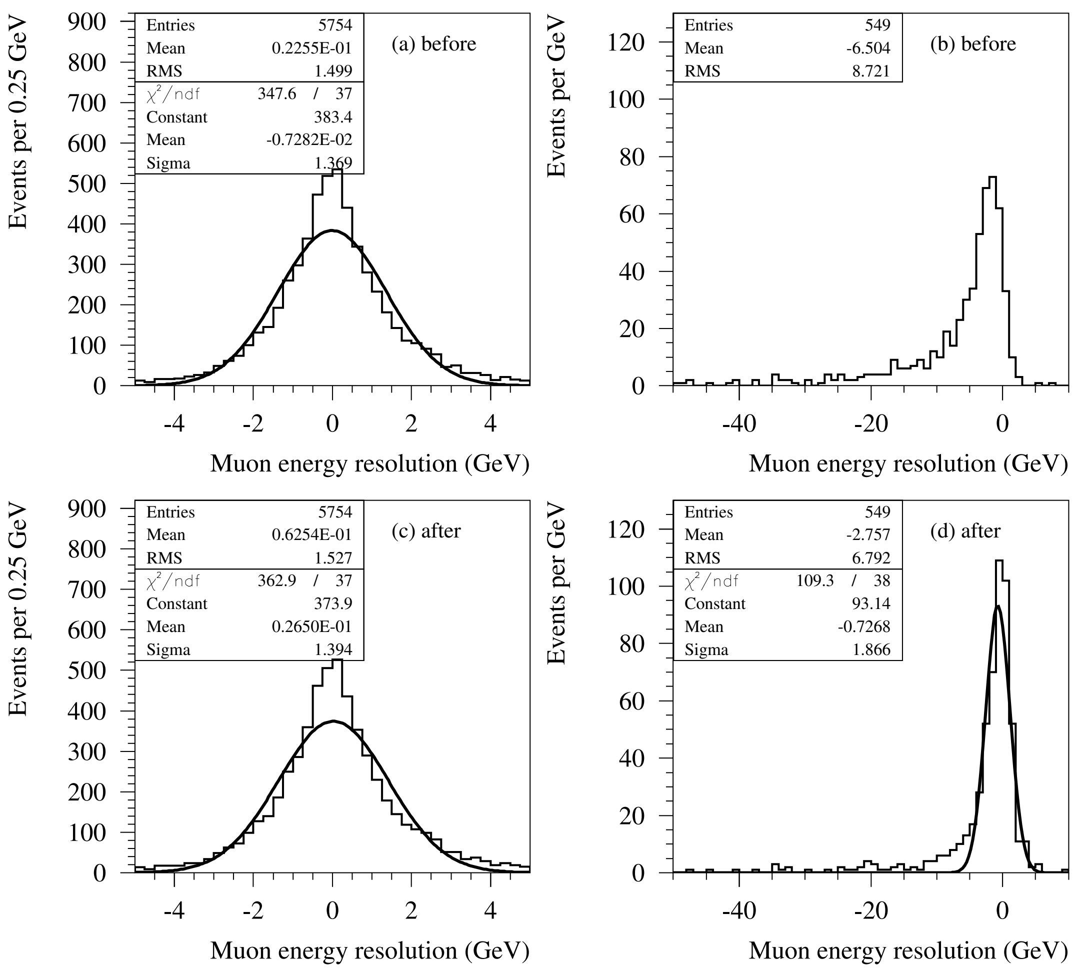

Figure 3.26: The resolution on the muon energy, in fully simulated and selected $\mu\bar{\nu}q\bar{q}$ events, before the FSR search for (a) events without any energy lost to photon radiation and (b) events with some energy lost to photon radiation. The corresponding resolutions after the FSR search are shown in (c) and (d).

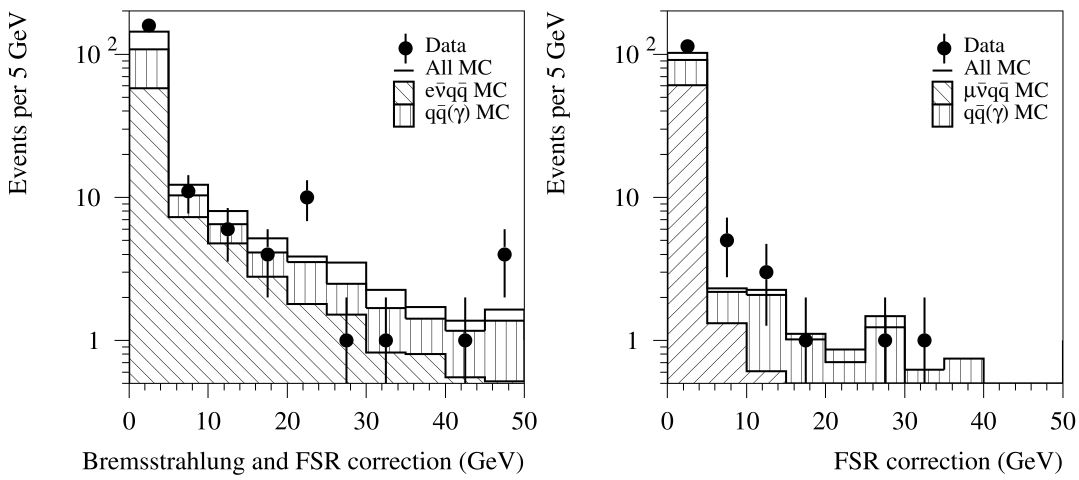

Figure 3.27: The energy added by the Bremsstrahlung correction and FSR search to (left) electrons and (right) muons for simulation and data.

3.2.6 Lepton energy.

The discriminating power between signal and background that is obtained from the lepton energy distribution, which is shown in Figure 3.28, is maximised by requiring the lepton energy to be at least 21 GeV. This keeps 99% of the signal semileptonic WW decays and rejects 73% of the $Z/\gamma \rightarrow q\bar{q}(\gamma)$ background in both the $e\bar{\nu}q\bar{q}$ and $\mu\bar{\nu}q\bar{q}$ channels. The increased rejection power for the $e\bar{\nu}q\bar{q}$ channel with respect to the $\sqrt{s} = 172$ GeV analysis is due to the requirement that the electron should be isolated for the Bremsstrahlung correction to be applied. Table 3.12 lists the efficiencies for all the signal and background processes.

3.2.7 Association of energy flow objects to the lepton.

In order to correctly reconstruct the two jets from the hadronic W decay, all objects associated to the lepton must be identified and removed from the list of energy flow objects used by the jet clustering algorithm. At $\sqrt{s} = 172$ GeV, the lepton charged track and any ECAL energy deposit associated by the Bremsstrahlung correction are excluded. However, the electron energy deposit may be partially in the HCAL, which creates a different kind of energy flow object, or the muon may deposit more energy in the calorimeters than expected, which creates an additional energy flow object. These energy flow objects should also be excluded.